

Experimental Demonstration of a Thermoacoustic Diode

Tetsushi Biwa, Hiroki Nakamura, and Hiroaki Hyodo

Department of Mechanical Systems and Design, Tohoku University, Sendai 980-8579, Japan
(Received 29 November 2015; revised manuscript received 7 March 2016; published 24 June 2016)

When an acoustic wave passes through short narrow channels in a regenerator having an axial temperature difference, the acoustic power is amplified for the waves going from cold to hot, whereas it is damped for the waves going in the opposite direction. This study applies such asymmetric wave propagation to demonstrate a thermoacoustic diode, which plays the role of the acoustic counterpart to an optical isolator. Four regenerators having the same longitudinal temperature difference are aligned in series to make four-stage amplification and damping of the acoustic power possible. This alignment leads to the enlarged difference between the acoustic power gains in the forward and backward propagation directions, even with a moderate temperature difference. Furthermore, by introducing the acoustical impedance-matching unit, the power-reflection coefficient is kept as low as 0.017 in forward propagation. The results show that the power-transmission coefficients in the forward and backward directions, respectively, reach 0.98 and 0.023, which means that the power-transmission ratio is 16 dB.

DOI: 10.1103/PhysRevApplied.5.064012

I. INTRODUCTION

Many studies have been undertaken to develop an *acoustic diode* that allows one directional propagation of acoustic waves [1–12]. In a uniform medium such as air or water, a plane acoustic wave can travel in forward and backward directions along a given channel. Installing an acoustic diode in such a channel, however, breaks transmission reciprocity. In other words, the acoustic wave is transmitted in the forward direction, but it is blocked in the backward direction. When the cross-sectional areas of the channels are equal for the incident and the transmitted waves, the power-transmission coefficient Γ is equivalent to the intensity-transmission coefficient [13]. Therefore, Γ is expressed as

$$\Gamma = \left| \frac{p_t}{p_i} \right|^2, \quad (1)$$

where p_i and p_t , respectively, stand for the complex amplitudes of the incident wave and the transmitted wave. Liang *et al.* [1] showed that the ratio $\Gamma_+ : \Gamma_-$ of the power-transmission coefficients for forward (+) and backward (−) directions reaches 40 dB in a system made by coupling a superlattice of water and glass with a layer of nonlinear medium of microbubble suspension. Li *et al.* [3] constructed a sonic crystal with a corrugated diffraction structure using steel rods. They obtained a contrast ratio of about 0.9, which corresponds to the power-transmission ratio $\Gamma_+ : \Gamma_- = 12.8$ dB.

The acoustic diode can be thought of as the acoustical counterpart of an optical isolator (also called an *optical diode*), which can ideally realize both $\Gamma_+ = 1$ and $\Gamma_- = 0$ without changing the frequency of the transmitted wave, for example, through the Faraday effect [14]. The acoustic

diodes, however, double the frequency of the transmitted wave [1,9] or greatly reduce the transmitted energy in the forward direction from the incident energy [3–6]. This study aims to develop an acoustic diode that can transmit the incident acoustic waves perfectly without reflection in the forward direction and block completely in the backward direction, by highlighting thermodynamic aspects of acoustic waves.

When the acoustic traveling wave passes through a positive temperature gradient imposed on a regenerator being a porous material with many narrow flow channels, the gas parcel experiences compression and expansion processes due to pressure oscillations and heating and cooling processes due to the displacement oscillations along the temperature gradient of the regenerator. Since the pressure and displacement oscillations of the gas parcel are out of phase by 90° in the traveling acoustic wave, the gas parcel undergoes a series of thermodynamic processes in the order of compression, heating, expansion, and cooling when the wave goes from cold to hot. The result of such a thermodynamic cycle being equivalent to the Stirling one, leads to the acoustic power amplification, whereas the gas parcel executes a reversed thermodynamic cycle resulting in acoustic power damping when the wave passes the regenerator from hot to cold [15,16]. The acoustic power gain G is given approximately by using p_i , p_t , and the complex amplitude p_r of the reflected wave as

$$G = \frac{|p_t|^2}{|p_i|^2 - |p_r|^2} \quad (2)$$

when the cross-sectional areas are the same at both the inlet and outlet sides. As Ceperley [17] has discussed theoretically, G is expected to reach the absolute

temperature ratio $T_{\text{out}}:T_{\text{in}}$ between temperature T_{out} in the outlet side over T_{in} in the inlet side if the isothermally reversible process is achieved between the gas and the solid walls in the regenerator while the viscous damping is small. Therefore, when the acoustic wave passes through the regenerator with different end temperatures, the regenerator acts as an acoustic power amplifier with $G > 1$ for the waves going up the temperature gradient, whereas it acts as an acoustic power damper with $G < 1$ for the waves going down the temperature gradient [18,19]. Furthermore, because the gas parcel experiences thermodynamic cycles locally within the range of its displacement oscillations, which is usually much smaller than the wavelength, this type of acoustic diode can have more acoustically compact length than other devices that rely on diffraction in periodic structures.

We design, build, and test the thermoacoustic diode made of the regenerator with a temperature gradient in this study. It is noteworthy that Γ is linked with G through the relation

$$\Gamma = (1 - |R|^2)G, \quad (3)$$

where

$$R = p_r/p_i \quad (4)$$

denotes the pressure-reflection coefficient. A nonzero R is brought about unavoidably by the regenerators because of the difference of the acoustic impedance from the intrinsic acoustic impedance of the gas. As we demonstrate later, we realize the thermoacoustic diode by inserting an impedance-matching unit that reduces the acoustic wave reflection.

II. EXPERIMENT

A. Experimental setup

A 20-mm-long regenerator is constructed by stacking many stainless-steel mesh screens with mesh number of 60 and 0.14-mm wire diameter, as presented in Fig. 1(a). The volume porosity of the regenerator is measured as 0.7. Therefore, the effective radius [20] of the regenerator pores is estimated as $r = 0.1$ mm. The regenerator is sandwiched by a hot heat exchanger and a cold heat exchanger, each of which is made of 10-mm-long brass parallel plates with spacing of 0.5 mm. The cold heat exchanger is cooled by running water, whereas the hot heat exchanger is heated steadily by an electrical heater wound around the hot heat exchanger. The temperatures T_C and T_H of cold and hot heat exchangers are monitored by thermometers. The regenerator unit consisting of the regenerator and two heat exchangers is inserted in an air-filled tube. The tube is made of a stainless-steel cylinder with 24-mm internal diameter and is 2.3 m long in total. A secondary cooling water pipe is wound around the tube 20 mm away from the hot heat

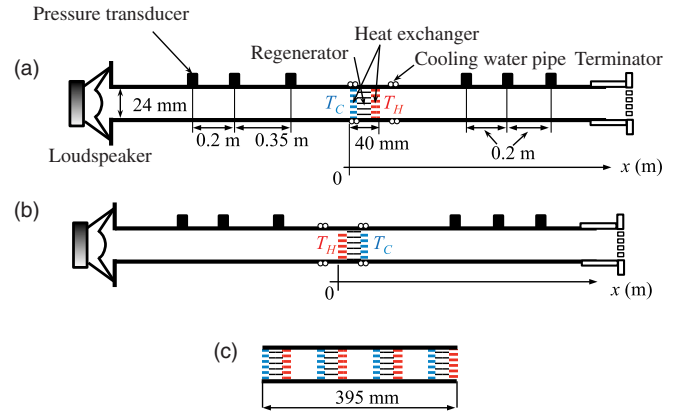


FIG. 1. Experimental setups with a single-stage regenerator for (a) the forward propagation and (b) backward propagation. The four-stage regenerator unit is shown in (c).

exchanger to make the air temperature in the tube remain at ambient temperature except for the region near the hot heat exchanger. The mean pressure is kept at atmospheric pressure (approximately 1×10^5 Pa).

A loudspeaker located at one end of the tube generates monofrequency acoustic oscillations with $f = 100.0$ Hz. The corresponding acoustic period (10.0 ms) is sufficiently longer than the thermal relaxation time $\tau \approx 0.3$ ms for the gas to equilibrate with the wall, where τ can be estimated as $\tau = r^2/(2\alpha)$ using the thermal diffusivity α of the gas [16]. This relation means that the gas parcel oscillates keeping good thermal contact with the screen wires in the regenerator used in this study and ensures the heating and cooling process without time delay relative to the displacement oscillations.

An acoustic terminator made from an air-filter material used for car engines is placed at the other end of the tube. We find that the terminator possesses the pressure-reflection coefficient with the magnitude of $(3.3 \pm 1.1) \times 10^{-2}$, which is sufficiently small in this study.

Figure 1(a) presents the experimental setup for the forward propagation where the sound waves go from cold to hot in the regenerator unit. For backward propagation, the regenerator unit orientation is reversed such that the acoustic waves go from hot to cold, as presented in Fig. 1(b). In this study, the axial coordinate x is consistently directed from the loudspeaker to the terminator; $x = 0$ is taken at the front of the regenerator unit. Therefore, the forward propagation and backward propagation, respectively, mean the wave propagations going up and down the temperature gradient. Additionally, it is noteworthy that the pressure-reflection coefficient R and the power-transmission coefficient Γ are determined using pressures at $x = 0$ and $x = L$, where L represents the regenerator unit length.

To achieve a higher gain with the same temperature difference, a four-stage regenerator unit is built by connecting four single-stage regenerator units in series, as presented in Fig. 1(c). All heat exchangers are controlled to

have the same T_H and T_C . The four-stage unit length is 395 mm, which is quite small compared with the wavelength ($= c/f \approx 3.4$ m; c is the speed of sound) of acoustic oscillations. Because of the four-stage amplification, the theoretical acoustic power gain is expected to become $G = (T_{\text{out}}:T_{\text{in}})^4$ instead of $G = T_{\text{out}}:T_{\text{in}}$ for the single-stage amplification.

B. Experimental method

As shown in Figs. 1(a) and 1(b), acoustic pressures are measured at three positions on both the speaker side and the terminator side with small pressure transducers flush mounted on the tube wall. Pressure signals, as well as the voltage signal of the function generator to drive the loudspeaker, are monitored using a spectrum analyzer. The amplitude and the phase difference relative to the voltage signal are determined from their Fourier spectra obtained from 16 384 data points for each signal. To ascertain the acoustic field from the measured pressures, we apply the so-called *two-sensor method* [21,22].

In the two-sensor method, acoustic pressure waves are decomposed into traveling waves going in the positive and negative directions of x . When the acoustic pressure of the angular frequency $\omega = 2\pi f$ is expressed as $P = p(x)\exp(i\omega t)$ with the imaginary unit i , the complex amplitude p is written as

$$p(x) = p_+e^{-ikx} + p_-e^{ikx}, \quad (5)$$

where k is a complex wave number for longitudinal acoustic oscillations of a gas confined in a channel. When the channel is a circular cylinder with radius r_0 , the wave number k is obtained analytically from the linear acoustic theory [23]. For a gas with the specific heat ratio γ , thermal diffusivity α , and kinematic viscosity ν , k is given as [16]

$$k = \frac{\omega}{c} \sqrt{\frac{1 + (\gamma - 1)\chi_\alpha}{1 - \chi_\nu}}, \quad (6)$$

where χ_j ($j = \alpha, \nu$) is expressed as

$$\chi_j = \frac{2J_1(Y_j)}{Y_j J_0(Y_j)}, \quad (7)$$

with

$$Y_j = (i - 1) \sqrt{\frac{\omega r_0^2}{2j}} \quad (8)$$

using Bessel functions J_0 and J_1 of the first kind. Under the present experimental conditions, the factor $\sqrt{[1 + (\gamma - 1)\chi_\alpha]/(1 - \chi_\nu)}$ in Eq. (6) is given as 1.02–0.014*i*.

Unknown complex constants p_\pm in Eq. (5) are determined experimentally from measurements of the complex pressure amplitudes p_A and p_B of two positions: $x = x_A$ and $x = x_B$. Because $p_A = p(x_A)$ and $p_B = p(x_B)$, we have the coupled equations

$$p_A = p_+e^{-ikx_A} + p_-e^{ikx_A}, \quad (9)$$

$$p_B = p_+e^{-ikx_B} + p_-e^{ikx_B}. \quad (10)$$

Solving these with respect to p_\pm gives

$$\begin{pmatrix} p_+ \\ p_- \end{pmatrix} = \frac{1}{e^{-ik\Delta} - e^{ik\Delta}} \begin{pmatrix} e^{ikx_B} & -e^{ikx_A} \\ -e^{-ikx_B} & e^{-ikx_A} \end{pmatrix} \begin{pmatrix} p_A \\ p_B \end{pmatrix}, \quad (11)$$

where $\Delta = x_A - x_B$. In this study, we determine the complex constants p_\pm on the speaker side as the average of those obtained from three pairs of the measured pressure. Similarly, we calculate p'_\pm on the terminator side from three pairs on the terminator side. The incident pressure amplitude p_i and the reflected pressure amplitude p_r both at $x = 0$, and the transmitted pressure amplitude p_t at $x = L$ are, respectively, given as

$$p_i = p_+, \quad (12)$$

$$p_r = p_-, \quad (13)$$

$$p_t = p'_+e^{-ikL}, \quad (14)$$

from which we evaluate Γ in Eq. (1) and R in Eq. (4).

The complex amplitude $v(x)$ of the cross-sectional average of the axial acoustic particle velocity is determined from the linearized Navier-Stokes equation, which is written as [16]

$$v(x) = \frac{i(1 - \chi_\nu)}{\omega \rho_m} \frac{dp(x)}{dx}, \quad (15)$$

where ρ_m denotes the temporal mean density of the gas. The complex factor $1 - \chi_\nu$ is evaluated as $0.98 + 0.018i$, which is close to unity. The acoustic power I is expressed as

$$I(x) = \frac{\pi r_0^2}{2} \text{Re}[p^\dagger(x)v(x)]. \quad (16)$$

Here, the symbol \dagger in Eq. (16) represents the complex conjugate. The acoustic powers $I(0)$ and $I(L)$ in the inlet and outlet sides of the regenerator unit are determined, respectively, using Eq. (16). Then, the acoustic power gain G is determined as

$$G = \frac{I(L)}{I(0)}. \quad (17)$$

We determine G from Eqs. (16) and (17) in this study, but G derived from Eq. (2) through Eqs. (12)–(14) gives a reasonable estimation within the relative error of 5% because the wave number k and the factor $1 - \chi_\nu$ are sufficiently close to ω/c and unity, respectively. The acoustic power I in Eq. (16) and, hence, the gain G in Eq. (17) are not influenced by the temperature gradient in the short pipe segment between the secondary cooling water pipe and the hot heat exchanger, as the pipe radius is too large to introduce thermoacoustic power amplification and damping. So we determine G , Γ , and R by neglecting the temperature gradient.

III. EXPERIMENTAL RESULTS

A. Thermoacoustic amplification

Figure 2 shows a log-log plot of the acoustic power gain G against the temperature ratio $T_{\text{out}}:T_{\text{in}}$. When the temperature ratio $T_{\text{out}}:T_{\text{in}} = 1$, the regenerator temperature is uniform at room temperature. The gain G of less than unity represents the acoustic power damping through the regenerator unit. As the slope shows, G approximately changes as a power of $T_{\text{out}}:T_{\text{in}}$ with the exponent of 1 in the single-stage unit, as predicted by Ceperley [17]. The gain G correspondingly exceeds unity when the wave propagates in the forward direction with $T_{\text{out}}:T_{\text{in}} \geq 2$. In contrast to energetically passive acoustic devices where the acoustic power damping or absorption is unavoidable [1,3–6,8,11], the present device can amplify the acoustic power as it is sourced from the thermodynamic cycle [17] associated with the positive temperature gradient. It is also readily apparent

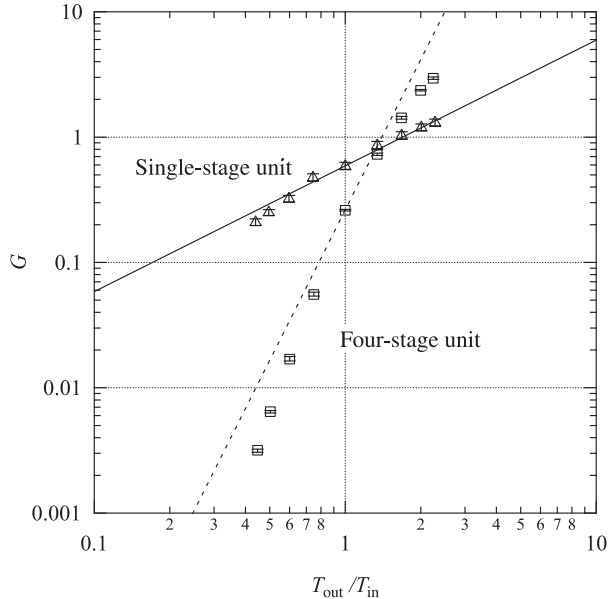


FIG. 2. Relation between the acoustic power gain G and the temperature ratio $T_{\text{out}}:T_{\text{in}}$ for the single-stage unit (triangle) and for the four-stage unit (square). Solid and dashed lines are drawn, respectively, to show slopes of 1 and 4.

that backward propagation results in a strong damping of $G = 0.23$, which can be attributed to the reversed cycle.

When the four-stage unit is adapted, the gain G changes its exponent to 4. The maximum G reaches 2.9 when $T_{\text{out}}:T_{\text{in}} = 2.3$. If one tries to obtain this value of G with a single-stage unit used in this study, then a rough extrapolation of G in Fig. 2 suggests that one will need the temperature ratio $T_{\text{out}}:T_{\text{in}}$ greater than 5, which means an impractically high temperature $T_H \geq 1500$ K when $T_C = 300$ K. Consequently, the use of a series configuration of the regenerators is effective for achieving a high-gain G_+ for forward propagation and a low-gain G_- for backward propagation with a modest temperature condition. In reality, the gain ratio $G_+:G_-$ reaches 927 ($= 30$ dB) with $T_H = 690$ K and $T_C = 310$ K.

Figures 3(a) and 3(b) show the acoustic field of $|p(x)|$ and $|v(x)|$ when the highest temperature ratio $T_H:T_C = 2.3$ is imposed on the four-stage unit, where Figs. 3(a) and 3(b), respectively, correspond to forward and backward propagations. The traveling wave field is evidenced by the axially uniform distribution of the acoustic amplitudes in the terminator side of the channel, irrespective of the

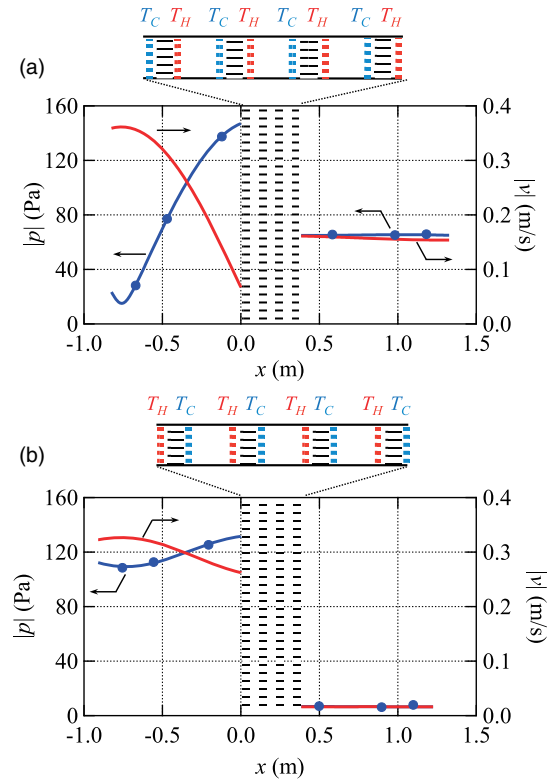


FIG. 3. Acoustic field of the pressure amplitude $|p|$ and the velocity amplitude $|v|$ in (a) forward propagation and (b) backward propagation. Symbols (filled circle) represent the measured pressure amplitudes. Stripes show the regenerator units. The blue curves for $|p|$ are obtained by inserting the experimental values of p_{\pm} into Eq. (5), and the red ones for $|v|$ are then given from Eq. (15).

propagation direction. In the loudspeaker side, however, a standing-wave-like field is created, particularly when the wave propagates in the forward direction, as manifested by a minimum of $|p|$ and a maximum of $|v|$ at $x = -0.76$ m. This acoustic field from the presence of a considerable amount of reflected waves from the four-stage regenerator unit. Indeed, the measured pressure-reflection coefficient is $R_+ = 0.83 - 0.25i$ for forward propagation, and the corresponding power-reflection coefficient $|R_+|^2$ is found to be 0.76, which means that a considerable fraction of the incident acoustic power is reflected by the four-stage unit. Although asymmetric wave propagation has already been realized in terms of $G_+ : G_-$, the ideal diode is expected to have zero reflection, at least in the forward propagation. As we describe in the next section, we try to install an acoustic device, which we call an impedance unit, to reduce the magnitude of the reflection coefficient R for forward propagation.

B. Thermoacoustic diode

To prevent acoustic reflection from the present four-stage regenerator unit, we adopt a technique used in electrical transmission lines. When the transmission line with the characteristic impedance Z_0 is terminated with an electrical element of the impedance $Z_e \neq Z_0$, the reflection takes place because of the impedance mismatch. To solve this problem, presuming that a series impedance Z_a and a parallel impedance Z_b are installed in front of Z_e , as portrayed in Fig. 4(a), then the additional impedances Z_a and Z_b change the terminating impedance of the transmission line to

$$Z = \frac{(Z_a + Z_b)Z_e + Z_a Z_b}{Z_b + Z_e}. \quad (18)$$

Therefore, when the combined impedance Z is adjusted to coincide with the characteristic impedance Z_0 by appropriate choice of Z_a and Z_b , the reflection can be perfectly

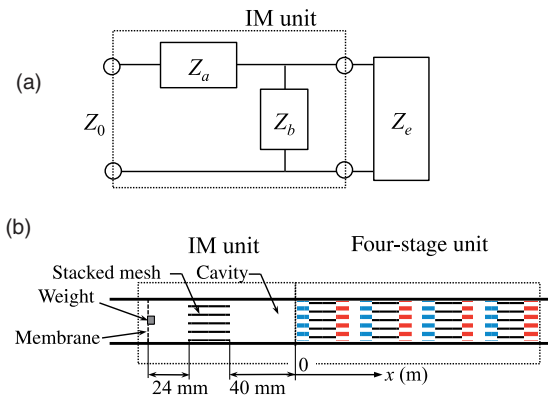


FIG. 4. Schematic diagram for the IM unit in the electrical transmission line (a) and the acoustic IM unit (b) inserted in front of the four-stage unit.

prevented. When such a condition is achieved, the electrical elements comprising Z_a and Z_b can be called an impedance-matching (IM) unit. Although we show the idea of the IM unit using the specific example presented in Fig. 4(a), various combinations of electrical elements are possible to achieve the same function.

Analogous discussion can be established between electrical elements and acoustical elements when ac voltage and current are regarded as, respectively, corresponding to pressure and volume velocity [13]. The total acoustic impedance of the present four-stage unit and the acoustic components on the back side of it is expressed by using experimental values of $p(0)$ and $v(0)$ as

$$Z = \frac{p(0)}{Av(0)}. \quad (19)$$

Consequently, if the acoustical IM unit is installed in front of the four-stage unit with the positive temperature gradient such that the combined impedance becomes equal to the characteristic acoustic impedance $\rho_m c/A$ of the cylindrical channel, then the reflection of the pressure waves should be diminished.

The IM unit used in this study consists of a 24 mm diameter and a 0.3-mm-thick silicone rubber membrane, a weight of 0.43 g glued onto the center of the membrane, a 24-mm-long stack of screen meshes (the mesh number is 40 and the wire diameter is 0.14 mm), and a cavity section between the stacked mesh and the four-stage unit. The spacings between the membrane and the stacked meshes are 24 mm, and the cavity length is 40 mm. These values are found to give the smallest reflection coefficient $|R_+|$ among those tested in preliminary measurements conducted with various combinations. The membrane and the stacked mesh screens constituting the impedance Z_a in Fig. 4 (a) provide an analogous inductance and resistance, whereas the cavity functions as an analogous capacitance as the parallel impedance Z_b . It is noteworthy that the length of the combined unit is 483 mm, still being less than 14% of the acoustic wavelength.

Shown in Fig. 5 are the reflection coefficients R_{\pm} for the forward and backward propagations when the IM unit is introduced, as well as those without the IM unit. To make the power-transmission ratio Γ_+ closer to unity, the temperature ratio is controlled to be 1.7 for the forward propagations based on the preliminary measurement on the acoustic power damping caused by the IM unit. The temperature ratio for the backward direction is accordingly set equal to 0.58 ($= 1/1.7$). It is readily apparent that R_+ comes close to the origin, which reflects the fact that $|R_+| = 0.87$ changes to $|R_+| = 0.13$ by introduction of the IM unit. Therefore, the power-reflection coefficient $|R_+|^2$ is reduced substantially from 0.76 to 0.017. Although the value of $|R_-|^2$ for the backward direction increases by the IM unit, it remains at the level of 0.063.

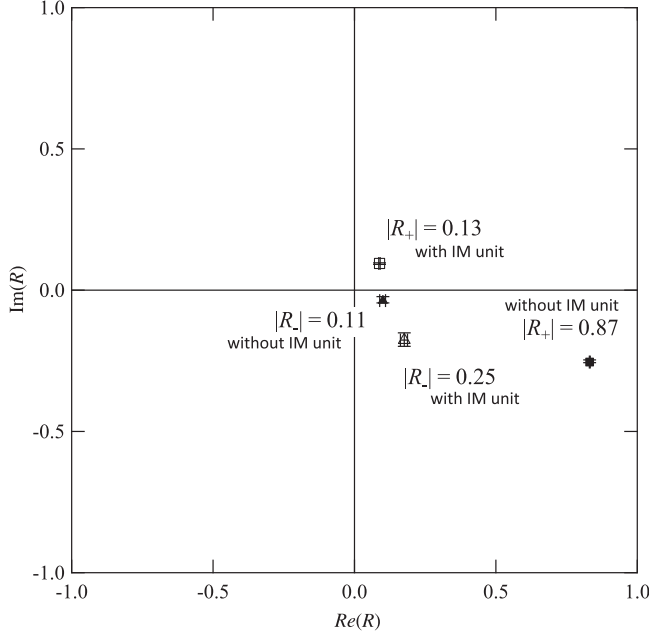


FIG. 5. Pressure-reflection coefficients R_{\pm} with the IM unit and without the IM unit. Subscripts \pm , respectively, represent the forward and backward propagation directions.

The improvement of the propagation characteristics is more visible in Fig. 6, where $|p|$ and $|v|$ are shown against the axial coordinate x for forward propagation. A comparison with those in Fig. 3(a) clearly illustrates the effectiveness of the IM unit, which contributes to the generation of the traveling wave field in the loudspeaker side, as well as in the terminator side, as shown by the uniform $|p|$ and $|v|$ in space. Now we are ready to present the propagation properties of the present acoustic diode made of the four-stage unit and the IM unit. From experiments, we obtain the power-reflection coefficient $|R_+|^2$, the acoustic power gain G , and the power-transmission coefficient Γ , as presented in Table I. It is apparent that the values of Γ , $|R|^2$, and G satisfy the relation in Eq. (3) in good accuracy. We achieve $\Gamma_+ = 0.98$ for the forward propagation and $|R_+|^2$ close to zero. Furthermore, Γ_- for the backward propagation is as small as 0.023. As a result, the ratio $\Gamma_+:\Gamma_-$ of the power-transmission coefficients reaches 16 dB because of the small value of Γ_- . Therefore, probably the present device fundamentally satisfies the conditions required for the acoustic diode. If a higher value for the ratio of $\Gamma_+:\Gamma_-$ is necessary, one just needs to increase the temperature ratio of the regenerator unit or the number of the regenerator units to more than four.

C. Frequency characteristic of the thermoacoustic diode

For a given regenerator, the thermoacoustic power amplification and damping are expected to occur in the frequency range satisfying $\omega\tau < 1$ [19]. As described in Sec. II A, the thermal relaxation time τ for the present

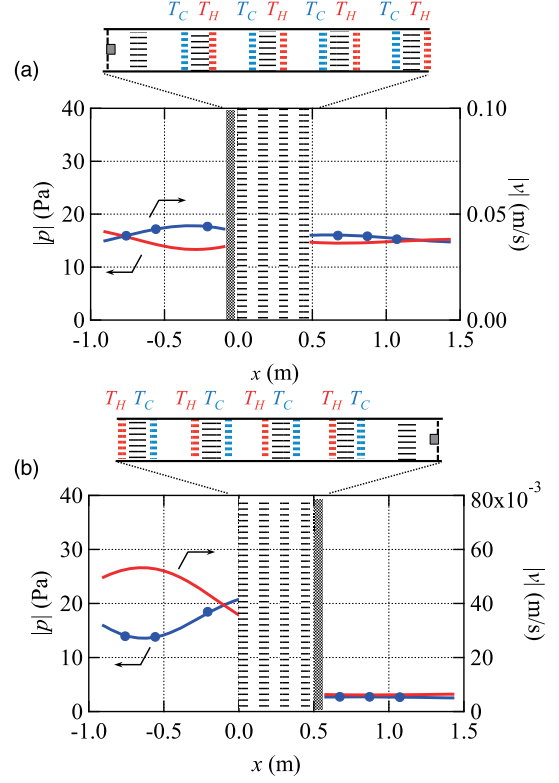


FIG. 6. Acoustic field of pressure amplitude $|p|$ and the velocity amplitude $|v|$ in forward propagation (a) and backward direction (b). Symbols (filled circle) represent the measured pressure amplitudes. Stripes and hatched areas show the regenerator units and the IM unit. The blue curves for $|p|$ are obtained by inserting the experimental values of p_{\pm} into Eq. (5), and the red ones for $|v|$ are then given from Eq. (15).

regenerator is estimated to be 0.3 ms. Thus, for the frequency range roughly below 500 Hz, the asymmetric acoustic power gain should be obtainable. The IM unit, on the other hand, should possess its own frequency characteristics depending on its construction. This section studies the frequency characteristics of the thermoacoustic diode presented in the previous section.

Figure 7(a) shows the power-transmission coefficients Γ_+ and Γ_- and also the power-reflection coefficients $|R_+|^2$ and $|R_-|^2$ of the thermoacoustic diode when the frequency of the acoustic wave is changed from 60 to 140 Hz. The temperature ratio $T_{\text{out}}:T_{\text{in}}$ is 1.7 in the forward propagation and 0.58 in the backward propagation. The power-transmission coefficient Γ_+ for the forward propagation shows a peak around $f = 100$ Hz and it decreases below 0.5 with $f \leq 85$ Hz and $f \geq 110$ Hz. This frequency dependence

TABLE I. Thermoacoustic diode propagation properties

	$ R ^2$	G	Γ
Forward	0.017	1.0	0.98
Backward	0.063	0.024	0.023

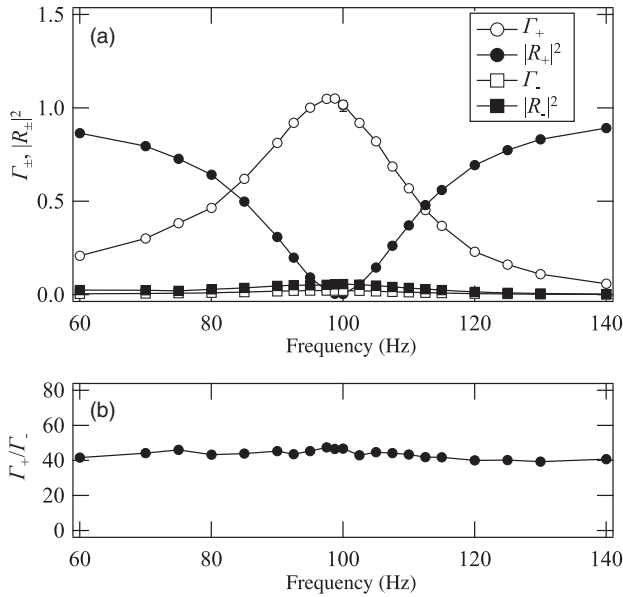


FIG. 7. Power-transmission coefficients Γ_+ and Γ_- , and power-reflection coefficients $|R_+|^2$ and $|R_-|^2$ measured in the frequency range from 60 Hz to 140 Hz (a) and power-transmission coefficient ratio $\Gamma_+:\Gamma_-$ (b).

reflects the increase of $|R_+|^2$ as f goes away from 100 Hz. Therefore, we see that the reflection of incident acoustic waves is kept small only in the frequency range near 100 Hz being the design frequency of the present IM unit.

For the backward propagation, $|R_-|^2$ is consistently smaller than 0.06, and Γ_- is also less than 0.02. Because of the smallness of the Γ_- values, we find the power-transmission ratio $\Gamma_+:\Gamma_-$ to be always greater than 40, as shown in Fig. 7(b). Therefore, the improvement of the IM unit will be a key point to expand the applicable frequency range of the thermoacoustic diode. If it is difficult to construct a desired IM unit in the whole frequency range of interest, one might be able to solve this problem by preparing several thermoacoustic diodes having different applicable frequency ranges and by arranging them in parallel. We are planning such a wide-band thermoacoustic terminator with a parallel configuration.

IV. SUMMARY

In summary, we experimentally demonstrate the thermoacoustic diode that allows one-way propagation of acoustic waves in the gas-confined tube with the power-transmission ratio of 16 dB. Acoustic power amplification and damping caused by thermodynamic asymmetry in the regenerator region play a central role in the present diode. The reflection from the regenerator unit is removed by the impedance-matching unit designed specifically for the regenerator unit. Realization of both the power-transmission coefficient as high as 0.98 and a reflection coefficient as low as 0.017 are characteristics of the present acoustic diode.

ACKNOWLEDGMENTS

The authors appreciate Professor Sam Hyeon Lee of Yonsei University for discussion at the early stage of the study and for providing us the acoustic terminator. This work is supported by JSPS KAKENHI (Grant No. 26286073).

- [1] B. Liang, X. S. Guo, J. Tu, D. Zhang, and J. C. Cheng, An acoustic rectifier, *Nat. Mater.* **9**, 989 (2010).
- [2] X. Zhu, X. Zou, B. Liang, and J. Cheng, One-way mode transmission in one-dimensional phononic crystal plates, *J. Appl. Phys.* **108**, 124909 (2010).
- [3] X. F. Li, X. Ni, L. Feng, M. H. Lu, C. He, and Y. F. Chen, Tunable Unidirectional Sound Propagation through a Sonic-Crystal-Based Acoustic Diode, *Phys. Rev. Lett.* **106**, 084301 (2011).
- [4] R. Li, B. Liang, Y. Li, W. Kan, X. Zou, and J. Cheng, Broadband asymmetric acoustic transmission in a gradient-index structure, *Appl. Phys. Lett.* **101**, 263502 (2012).
- [5] H. Sun, S. Zhang, and X. Shui, A tunable acoustic diode made by a metal plate with periodical structure, *Appl. Phys. Lett.* **100**, 103507 (2012).
- [6] Y. Li, J. Tu, B. Linag, X. Guo, D. Zhang, and J. C. Cheng, Unidirectional acoustic transmission based on source pattern reconstruction, *J. Appl. Phys.* **112**, 064504 (2012).
- [7] B. I. Popa, L. Zigoneanu, and S. A. Cummer, Tunable active acoustic metamaterials, *Phys. Rev. B* **88**, 024303 (2013).
- [8] Y. Li, B. Liang, Z. Gu, Z. Zou, and J. C. Cheng, Unidirectional acoustic transmission through a prism with near-zero refractive index, *Appl. Phys. Lett.* **103**, 053505 (2013).
- [9] B. Popa and S. Cummer, Non-reciprocal and highly non-linear active acoustic metamaterials, *Nat. Commun.* **5**, 3398 (2014).
- [10] R. Fleury, D. Sounas, C. Sieck, M. Haberman, and A. Alu, Sound isolation and giant linear nonreciprocity in a compact acoustic circulator, *Science* **343**, 516 (2014).
- [11] C. Liu, Z. Du, Z. Sun, H. Gao, and X. Guo, Frequency-Preserved Acoustic Diode Model with High Forward-Power-Transmission Rate, *Phys. Rev. Applied* **3**, 064014 (2015).
- [12] T. Devaux, V. Tournat, O. Richoux, and V. Pagneux, Asymmetric Acoustic Propagation of Wave Packets via the Self-Demodulation Effect, *Phys. Rev. Lett.* **115**, 234301 (2015).
- [13] L. E. Kinsler, A. R. Frey, A. B. Coppers, and J. V. Sanders, *Fundamentals of Acoustics* (Wiley, New York, 2000).
- [14] A. Maznev, A. Every, and O. Wright, Reciprocity in reflection and transmission: What is a phonon diode, *Wave Motion* **50**, 776 (2013).
- [15] G. W. Swift, *Thermoacoustics: A unifying perspective for some engines and refrigerators* (Acoustical Society of America, Sewickley, PA, 2002).
- [16] A. Tominaga, Thermodynamic aspects of thermoacoustic theory, *Cryogenics* **35**, 427 (1995).
- [17] P. H. Ceperley, Pistonless Stirling engine: Traveling wave heat engine, *J. Acoust. Soc. Am.* **66**, 1508 (1979).

- [18] T. Biwa, Y. Tashiro, U. Mizutani, M. Kozuka, and T. Yazaki, Experimental demonstration of thermoacoustic energy conversion in a resonator, *Phys. Rev. E* **69**, 066304 (2004).
- [19] T. Biwa, R. Komatsu, and T. Yazaki, Acoustical power amplification and damping by temperature gradients, *J. Acoust. Soc. Am.* **129**, 132 (2011).
- [20] Y. Ueda, T. Kato, and C. Kato, Experimental evaluation of the acoustic properties of stacked-screen regenerators, *J. Acoust. Soc. Am.* **125**, 780 (2009).
- [21] A. M. Fusco, W. C. Ward, and G. W. Swift, Two-sensor power measurements in lossy ducts, *J. Acoust. Soc. Am.* **91**, 2229 (1992).
- [22] T. Biwa, Y. Tashiro, H. Nomura, Y. Ueda, and T. Yazaki, Experimental verification of a two-sensor acoustic intensity measurement in lossy ducts, *J. Acoust. Soc. Am.* **124**, 1584 (2008).
- [23] H. Tijdeman, On the propagation of sound waves in cylindrical tubes, *J. Sound Vib.* **39**, 1 (1975).